

SCARLET-NAS: Bridging the gap between Stability and Scalability in Weight-sharing Neural Architecture Search

Xiangxiang Chu¹, Bo Zhang¹, Jixiang Li¹, Qingyuan Li², Ruijun Xu¹

¹Xiaomi AI Lab

²Xiaomi IoT

{chuxiangxiang, zhangbo11, lijixiang, liqingyuan, xuruijun}@xiaomi.com

Abstract

To discover compact models of great power is the goal of neural architecture search. Previous one-shot approaches are limited by fixed-depth search spaces. Simply paralleling skip connections with other choices can make depths variable. Unfortunately, it creates a large range of perturbation for supernet training, which makes it difficult to evaluate models. In this paper, we unveil its root cause under single-path settings and tackle the problem by imposing an *equivariant learnable stabilizer* on each skip connection. It has threefold benefits: improved convergence, more reliable evaluation, and retained equivalence. The third benefit is of the utmost importance for scalability. As appending stabilizers to a model doesn't change its representational capacity, we can now evaluate the stabilized counterpart as an identical proxy. With an evolutionary search backend that treats the supernet as an evaluator, we derive a family of state-of-the-art architectures, the SCARLET¹ series, at a tremendously reduced cost compared with EfficientNet. Our models are published here².

1 Introduction

Incorporating scalability into neural architecture search is the key to exploring efficient networks. The handcrafted way of scaling models up and down is to stack more or fewer cells [He *et al.*, 2016; Zoph *et al.*, 2018]. However, model scaling is nontrivial which involves tuning width, depth, and resolution altogether. To this end, a compound scaling method is then proposed in [Tan and Le, 2019], but it starts with a mobile baseline and 'grid-search' the combination of these three factors to achieve larger models. In this paper, we concern mainly about smaller models with a fixed input resolution and we focus on modifying the depth only.

A simple thought is to construct a search space of variable depths. Skip connections are widely used to cut down the depth in differentiable approaches [Cai *et al.*, 2019; Wu *et al.*, 2019]. But they face a common issue of undesired

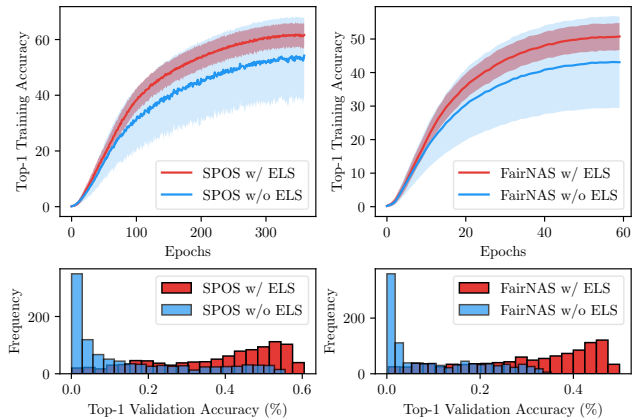


Figure 1: Training supernet with Single Path One-Shot [Guo *et al.*, 2019] and FairNAS [Chu *et al.*, 2019] on ImageNet with and without Equivariant Learnable Stabilizer (ELS) in search space S_1 . **Top:** The supernets with ELS enjoy better convergence (red thick lines) and small variance (red shaded area). **Bottom:** Histogram of randomly sampled 1k one-shot models' accuracies.

skip connection aggregation as noted by [Chen *et al.*, 2019; Zela *et al.*, 2019], which yields non-optimal results. Recent advances in one-shot approaches take a two-stage mechanism: single-path supernet optimization and searching [Guo *et al.*, 2019; Chu *et al.*, 2019]. This could potentially avoid the aggregation problem but they carefully removed skip connections from search spaces. To achieve our goal, we integrate skip connections under single-path settings because they are more efficient and less error-prone.

Our contributions can be summarized as follows,

Firstly, we disclose the training instability (see Figure 1) when skip connections are enabled in common search spaces. Beyond that, we uncover its root cause that similarities of features across different choices are broken by skip connections.

Secondly, we propose a simple learnable stabilizer to restore the stability in supernet training. We prove that the representational power is invariant under such transformation. The stabilized supernet is scalable in terms of searching models of variable depths.

Lastly, with the stabilized scalable supernet at hand, we perform a single proxyless evolutionary search on ImageNet at the cost of **10 GPU days**. Three new state-of-the-art mod-

¹SCALable supeRnet with Learnable Equivariant sTablizer

²<https://github.com/xiaomi-automl/SCARLET-NAS>

els of different depths are found, especially SCARLET-A scores **76.9%** on ImageNet with fewer FLOPs than EfficientB0. Moreover, we manually scale the searched models to have the same FLOPs with upscaled EfficientNet variations and we also obtain comparable results.

2 Preliminary Background

2.1 Single-Path Supernet Training

The weight-sharing mechanism is now widely applied in *neural architecture search* to save time [Pham *et al.*, 2018; Liu *et al.*, 2019; Bender *et al.*, 2018]. It is usually embodied as a supernet that incorporates all subnetworks. The supernet is trained till convergence only once, from which all subnetworks (also called *one-shot models*) can inherit weights for evaluation without extra fine-tuning. It is thus named the *one-shot* approach, as opposed to those who train each child network independently [Zoph *et al.*, 2018; Tan *et al.*, 2019]. Methods vary on how to train the supernet. In this paper, we concentrate on the single-path way [Guo *et al.*, 2019; Chu *et al.*, 2019], which is more memory-friendly and efficient.

Single Path One-Shot [Guo *et al.*, 2019] utilizes a supernet \mathcal{A} with 20 layers, and there are 4 choice blocks per layer based on ShuffleNet [Zhang *et al.*, 2018]. The total size of the search space reaches 4^{20} . It uniformly samples a single-path model (say a with weights W_a) to train at each step, after which only this activated path in the supernet gets its weights W_a updated. Formally, this process is to reduce the overall training loss \mathcal{L}_{train} of the supernet,

$$W_{\mathcal{A}} = \operatorname{argmin}_W \mathbb{E}_{a \sim \Gamma_{\mathcal{A}}} [\mathcal{L}_{train}(\mathcal{A}(a, W_a))] \quad (1)$$

Notice that it differs from the nested manner in differential approaches [Liu *et al.*, 2019; Dong and Yang, 2019] where Γ is not fixed but used as a representation for variable architectural weights.

FairNAS [Chu *et al.*, 2019] rephrases each supernet training step as training m single-path models either sequentially or in parallel. These models are built on choice blocks *uniformly sampled without replacement* (denoted as $a \sim \Psi_{\mathcal{A}}$). During each step, all blocks in the supernet are trained once. The weights are aggregated and also updated once in a single step. It can be formulated as,

$$W_{\mathcal{A}} = \operatorname{argmin}_W \mathbb{E}_{a \sim \Psi_{\mathcal{A}}} \left[\frac{1}{m} \sum_i^m \mathcal{L}_{train}(\mathcal{A}(a_i, W_{a_i})) \right] \quad (2)$$

By ensuring the same amount of training for each block, FairNAS achieves an obvious improvement in supernet performance. Interestingly enough, features learned by each block (of the same layer) in thus-trained supernet have high channel-wise similarities³. This will be later proved a useful hint to restore training stability when skip connections are involved.

³Cosine similarities are above 0.92 by average.

2.2 Search Spaces

For later experiments, we add skip connections to two common search spaces S_1 and S_2 described as follows,

Search Space S_1 . It is similar to ProxylessNAS [Cai *et al.*, 2019], where MobileNetV2 [Sandler *et al.*, 2018] is adopted as its backbone. In particular, S_1 is represented as a block-level supernet with $L = 19$ layers of $N = 7$ choices each. Its total size is 7^{19} . The choices are,

- MobileNetV2’s inverted bottleneck blocks [Sandler *et al.*, 2018] of two expansion rates (x) in (3,6), three kernel sizes (y) in (3,5,7), labelled as MBE xKy^4 ,
- skip connection (the 6th choice⁵).

Search Space S_2 . On top of S_1 , we give each inverted bottleneck a squeeze-and-excitation [Hu *et al.*, 2018] option (e.g., ExKy, ExKy-SE), similar to MnasNet [Tan *et al.*, 2019]. Its total size thus becomes 13^{19} .

We have to notice that *skip connections* are commonly used [Tan *et al.*, 2019; Liu *et al.*, 2019; Bender *et al.*, 2018], but meticulously neglected in recent single-path one-shot methods [Guo *et al.*, 2019; Chu *et al.*, 2019]. This is however not a trivial decision. Later we show that including skip connections makes trouble for supernet training and also largely influences its ranking ability.

3 Training Instability and a Cure

3.1 Skip Connections Trouble Supernet Training

The skip connection plays an important role in changing depths for architectures searched in block-level search spaces like S_1 and S_2 . To investigate *scalability* in one-shot approaches, we train the supernet in a single-path fashion (as discussed in Section 2.1) in search space S_1 where skip connections are included. Surprisingly, we find them bringing about severe **training instability**, which is illustrated in Figure 1. Unlike the reported stable training process of low variances [Guo *et al.*, 2019; Chu *et al.*, 2019], we instead observe much higher variances (shadowed in blue at the top of Figure 1) and lower training accuracies (blue line).

Training instability also deteriorates one-shot model performance. We sample 1024 models to measure their accuracies on ImageNet validation dataset. A majority of models from both SPOS (bottom left in blue) and FairNAS (bottom right in blue) are located in a wide range with low accuracies. This phenomenon hasn’t been observed in reduced S_1 (without skip connections) by previous works.

3.2 Analysis of Training Instability

A well-trained supernet matters for one-shot models’ ranking. We are thus driven to unveil what causes such a phenomenon to find a cure for stabilizing the training process.

Inspired by the analysis of the underlying working mechanism in the single-path training [Chu *et al.*, 2019], we pick the third layers of the formerly trained supernet to calculate cosine similarities across different choice blocks and depict the

⁴The order of numbering $o = (x - 3) + (y - 3)/2$.

⁵zero-based numbering

7×7 similarity matrix in Figure 2. The first six inverted bottlenecks of different configurations have quite similar high-dimension features ($32 \times 28 \times 28$) and their cosine similarities are higher (above 0.85). Meanwhile, the feature maps of the skip connection (the last choice block) are much more different from any one of them and the average cosine similarity is below 0.6. This disparity is observed in both training methods.

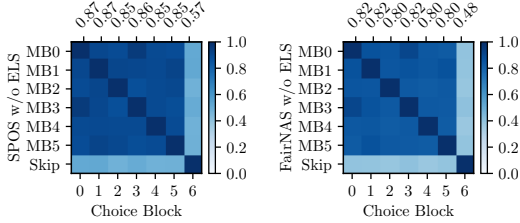


Figure 2: Cosine similarity matrix of the third layer’s outputs (averaged on 32 channels of 28×28 feature maps) from 7 choice blocks of supernet without ELS. The average similarity is shown as x -axis at the top. The skip connection yields quite different feature maps than others. **Left:** Single Path One-Shot [Guo *et al.*, 2019], **Right:** FairNAS [Chu *et al.*, 2019].

This comes as no surprise. During the single-path training, as the fourth layer randomly selects one output from the third layer, the unique skip connection brings in much stronger *feature augmentation* than others with higher similarities. This discrepancy of inflowing features (occurs in many layers) deteriorates supernet training, which has been shown on the top of Figure 1. As an outcome, large variances make big trouble to predict submodels’ performance. Under this condition, the supernet is nearly useless because it severely underestimates or overestimates candidate architectures, shown at the bottom of Figure 1. Therefore, we attribute the instability to low similarities of features across different paralleled choices, mainly from skip connections.

3.3 Improve Supernet Training with a Learnable Stabilizer

Based on the previous discussion, one direct approach to stabilize the training process is boosting the cross-block similarities by replacing the *parameter-free* skip connection with a learnable stabilizer. Ideally, the stabilizer will deliver similar features as other choice blocks. Beyond this, the stabilizer needs to comply with one crucial requirement for consistency: *The submodel with a plug-in learnable stabilizer must be exactly equivalent, regarding representational capacity, to the one without it.* A stabilizer satisfying this requirement is then called an Equivariant Learnable Stabilizer (ELS).

For a search space S like S_1 with n choices per layer, we denote $x_l^{c_l}$ as the input with c_l channels to layer l , and f_l^o the o -th operation function in that layer. Without loss of generality, the skip connection is the last choice (ordered $n - 1$) and other choices start with a convolution operation⁶. The

⁶ 1×1 for the inverted bottleneck block without skip connections in case of channel mismatch.

equivalence requirement for an equivariant learnable stabilizer function f_l^{ELS} can then be formulated as,

$$f_{l+1}^o(x_l^{c_l}) = f_{l+1}^o(f_l^{ELS}(x_l^{c_l})), \forall o \in \{0, 1, 2, \dots, n-1\}. \quad (3)$$

As for S , we can utilize the property of matrix multiplication to find a simple ELS function: a 1×1 convolution with c_l input channels and c_{l+1} output ones without batch normalization or activation, which is proven below.

Lemma 1. Let $f_l^{ELS} = Conv_{(c_l, c_{l+1}, 1, 1)}$, then Equation 3 holds.

Proof. First, we prove that Equation 3 holds for $\forall o \in \{0, 1, 2, 3, \dots, n - 2\}$. In this case, it’s sufficient to prove the output of the first convolution $Conv_{(c_l, m, k, k)}$ can be exactly matched by adding $Conv_{(c_l, c_{l+1}, 1, 1)}$ before $Conv_{(c_{l+1}, m, k, k)}$. Let $W_{c_l, c_{l+1}, 1, 1}^1$ and $W_{c_l, m, k, k}^2$ be the weight tensors of $Conv_{(c_l, c_{l+1}, 1, 1)}$ and $Conv_{(c_{l+1}, m, k, k)}$. Let $W_{c_l, m, k, k}^3$ be the weight tensors of $Conv_{(c_l, m, k, k)}$. Let w be one element of the tensor.

$$y = Conv_{(c_l, c_{l+1}, 1, 1)}(x_l^{c_l}), z = Conv_{(c_{l+1}, m, k, 1)}(y)$$

$$y(i, j, c) = \sum_{p=1}^{c_l} w_{p, c, 1, 1}^1 x(i, j, p)$$

Also,

$$\begin{aligned} z(i, j, c) &= \sum_{q=1}^k \sum_{p=1}^{c_{l+1}} w_{p, c, q, q}^2 y(i + q, j + q, p) \\ &= \sum_{q=1}^k \sum_{p=1}^{c_{l+1}} w_{p, c, q, q}^2 \left(\sum_{u=1}^{c_l} w_{u, p, 1, 1}^1 x(i + q, j + q, u) \right) \\ &= \sum_{q=1}^k \sum_{p=1}^{c_{l+1}} \sum_{u=1}^{c_l} w_{p, c, q, q}^2 w_{u, p, 1, 1}^1 x(i + q, j + q, u) \\ &= \sum_{q=1}^k \sum_{u=1}^{c_l} w_{u, c, q, q}^3 x(i + q, j + q, u) \end{aligned}$$

Therefore, the first part is proved by setting

$$w_{u, c, q, q}^3 = \sum_{p=1}^{c_{l+1}} w_{p, c, q, q}^2 w_{u, p, 1, 1}^1.$$

For $o = n - 1$, we replace a skip connection with an ELS. We can iteratively apply the first part of the proof till the end of searchable layers, which is also followed by a convolution. \square

Based on this proof, we now can expect improved stability in supernet training by adopting 1×1 convolution as an ELS while maintaining equivariance. Once the supernet is trained, we are allowed to better evaluate any sampled path (including the ones with ELS) with inherited weights. Scalability is achieved by removing ELS while retaining the same representational power.

4 Neural Architecture Search with Stabilized Supernet

One-shot approaches [Bender *et al.*, 2018; Guo *et al.*, 2019; Chu *et al.*, 2019] divide neural architecture search into two stages: supernet training and searching. In Section 3 we have shown the first part. For the second stage, previous methods apply either random search or evolutionary algorithms. It is however nontrivial when skip connections are included. First of all, in an evolutionary search pipeline like that of [Chu *et al.*, 2019], three objectives like classification accuracies, multiply-adds and the number of parameters are of different importance. We concern more about accuracies (performance) and multiply-adds (speed) than number of parameters (memory). This calls for a weighted solution. Second, models with too many skip connections can easily stand out because of low multiply-adds. This is not desired as such a model dominates others but comes with a low accuracy. Third, as we care for mobile deployment, we should encourage increasing the number of parameters to prevent underfitting rather than overfitting [Zhang *et al.*, 2018]. Last, for practical reasons, we need to set a minimum accuracy acc_{min} and maximum multiply-adds $madds_{max}$. Formally, we describe the searching process as,

$$\begin{aligned} &max \quad \{acc(m), -madds(m), params(m)\} \\ &s.t. \quad m \in \text{search space } S \\ &\quad w_{acc} + w_{madds} + w_{params} = 1, \forall w \geq 0 \\ &\quad acc(m) > acc_{min}, madds(m) < madds_{max}. \end{aligned} \quad (4)$$

Specifically, we adopt a similar evolutionary searching algorithm based on NSGA-II [Deb *et al.*, 2002] as in FairNAS [Chu *et al.*, 2019] with some modifications. For handling weights of different objectives, we make use of weighted crowding distance [Friedrich *et al.*, 2011] to facilitate non-dominated sorting. We set $w_{acc} = 0.4, w_{madds} = 0.4, w_{params} = 0.2$. The constraints are set to $madds_{max} = 500M$ and $acc_{min} = 0.4$. Notice that we treat these two constraints in sequential order to reduce cost. As calculating multiply-adds is much faster than accuracies, models violating $madds_{max}$ are immediately removed for further evaluation. In summary, our search pipeline is presented in Algorithm 1.

In total, the evolution covered 8400 models (70 models each for 120 generations). It costs 12 GPU days on a Tesla V100. The final architectures SCARLET-A, B and C are sampled from the Pareto front and are trained from scratch. Due to the equivalence requirement, we remove ELS to achieve two competitive models with shorter depths, SCARLET-B and C. This proves that our stabilized supernet can make reliable evaluation even when skip connections are involved.

5 Experiments

5.1 Dataset and Training Details

Dataset. Throughout the paper, we always use the ILSVRC2012 dataset [Deng *et al.*, 2009]. To be consistent with previous works [Tan *et al.*, 2019], the validation set consists of 50k images selected from the training set. The original validation set serves as the test set instead.

Algorithm 1 The constrained and weighted NAS pipeline.

Input: Supernet S , the number of generations N , population size n , validation dataset D , constraints C , objective weights w

Output: A set of K individuals on the Pareto front.

Train supernet S defined on the scalable search space.

Uniformly generate the populations P_0 and Q_0 until each has n individuals satisfying $C_{FLOPs}, C_{Accuracy}$.

for $i = 0$ **to** $N - 1$ **do**

$R_i = P_i \cup Q_i$

$F = \text{non-dominated-sorting}(R_i)$

Pick n individuals to form P_{i+1} by ranks and the crowding distance **weighted** by w .

$Q_{i+1} = \emptyset$

while $size(Q_{i+1}) < n$ **do**

$M = \text{tournament-selection}(P_{i+1})$

$q_{i+1} = \text{crossover}(M) \cup \text{hierarchical-mutation}(M)$

{Check the FLOPs constraint at first (It takes $< 1ms$).}

if $FLOPs(q_{i+1}) > FLOPs_{max}$ **then**

continue

end if

Evaluate model q_{i+1} with S on D {Check the accuracy constraint (It takes $\approx 60s$).}

if $Accuracy(q_{i+1}) > Acc_{min}$ **then**

Add q_{i+1} to Q_{i+1}

end if

end while

end for

Select K equispaced models near Pareto-front from P_N

Supernet Training. For FairNAS’s supernet of S_1 , we follow [Chu *et al.*, 2019] except that we train it for 60 epochs. It costs nearly 10 GPU days. For SPOS’s supernet of S_1 , we train it for 360 epochs to have the same amount of weight updates per block. As for S_2 with more choices, we use the same setting except for a smaller batch size of 256, i.e. more back-propagation iterations, which results in a supernet with higher top-1 accuracy on average.

Single Model Training. To train the selected single model, we follow MnasNet [Tan *et al.*, 2019] with vanilla Inception preprocessing [Szegedy *et al.*, 2017]. We train EfficientNet and SCARLET models without AutoAugment [Cubuk *et al.*, 2018] to have a fair comparison with state-of-the-art architectures. The batch size is 4096. The initial learning rate is 0.256 and it decays at an amount of 0.01 every 2.4 epochs. The dropout with a rate 0.2 [Srivastava *et al.*, 2014] is put before the last FC layer. The weight decay rate (l_2) is $1e - 5$. The RMSProp optimizer has a momentum of 0.9.

5.2 Comparison of State-of-the-art Architectures

After a single proxyless search in S_2 , we select three models (named SCARLET-A, B and C) from the Pareto front with equal distance. The architectures are illustrated in Figure 3. Table 1 shows a comparison with state-of-the-art classification models. Although in absence of AutoAugment tricks [Cubuk *et al.*, 2018], SCARLET-A still clearly surpasses EfficientNet-B0 (+0.6% higher top-1 accuracy) using

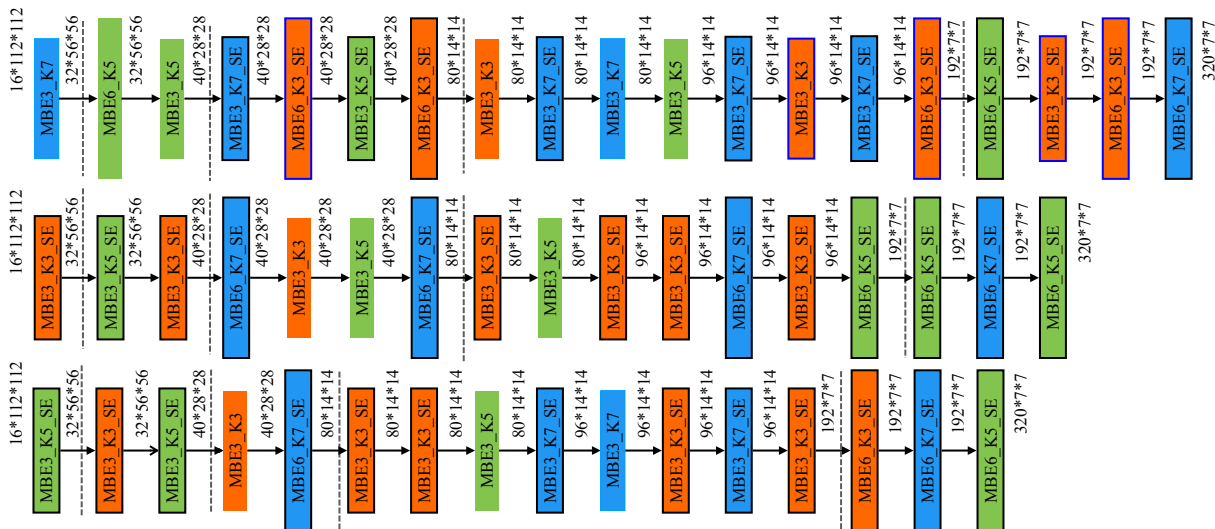


Figure 3: The architectures of SCARLET-A, B and C (from top to bottom). Downsampling points are indicated by dashed lines. Note the stem and tail parts are not drawn for simplicity.

| Models | $\times +$ (M) | Params (M) | Top-1 (%) | Top-5 (%) |
|-----------------------------|-------------------|---------------|--------------|--------------|
| MobileNetV2 [2018] | 300 | 3.4 | 72.0 | 91.0 |
| MobileNetV3 [2019] | 219 | 5.4 | 75.2 | 92.2 |
| MnasNet-A1 [2019] | 312 | 3.9 | 75.2 | 92.5 |
| MnasNet-A2 [2019] | 340 | 4.8 | 75.6 | 92.7 |
| FBNet-B [2019] | 295 | 4.5 | 74.1 | - |
| Proxyless-R [2019] | 320 | 4.0 | 74.6 | 92.2 |
| Proxyless GPU [2019] | 465 | 7.1 | 75.1 | - |
| Single-Path [2019] | 365 | 4.3 | 75.0 | 92.2 |
| Single Path One-Shot [2019] | 328 | 3.4 | 74.9 | 92.0 |
| FairNAS-A [2019] | 388 | 4.6 | 75.3 | 92.4 |
| EfficientNet B0 [2019] | 390 | 5.3 | 76.3 | 93.2 |
| SCARLET-A (Ours) | 365 | 6.7 | 76.9 | 93.4 |
| SCARLET-B (Ours) | 329 | 6.5 | 76.3 | 93.0 |
| SCARLET-C (Ours) | 280 | 6.0 | 75.6 | 92.6 |

Table 1: Comparison with state-of-the-art architectures on the classification task in ILSVRC 2012.

fewer FLOPs. The shallower model SCARLET-B achieves 76.3% top-1 accuracy with 329M FLOPs, which exceeds several models of similar size with a clear margin: MnasNet-A1 (+1.1%), Proxyless-R (+1.7%). Notably, to be comparable to our shallowest model SCARLET-C (75.6%), MnasNet-A1 comes with 21% more FLOPs at the cost of $200\times$ GPU days.

5.3 Free Manual Upscaling

We also consider higher accuracy requirements beyond mobile settings. To be comparable with EfficientNet’s scaled variants, we simply manually upscale our SCARLET baseline models to have the same resolution and FLOPs without any extra tuning cost. We compared the results with other state-of-the-art methods in Table 2.

At the level of 1 billion FLOPs, while EfficientNet-B2 is

based on grid search at a very high cost on GPUs [Tan and Le, 2019], our SCARLET-A2 achieves 79.5% top-1 accuracy for free. No AutoAugment tricks are applied regarding fairness. Moreover, Xception [Chollet, 2017] uses 8 times more FLOPs to reach 79.0%. Notably, our SCARLET-A4 achieves new state-of-the-art top-1 accuracy 82.3% again without extra costs using only 4.2 billion FLOPs. By contrast, SENet [Hu *et al.*, 2018] uses 9 times more FLOPs.

6 Ablation Study and Analysis

6.1 Training Stability

In Section 3, we expect that ELS can help stabilize the training of supernet with skip connections. We show its results in Figure 4. Cross-block features have higher channel-wise similarities when ELS is enabled (boosted about 0.3 for skip connections). We also illustrate feature vectors (in arrows) with angles (in shades) in the right column where the one with ELS enabled have much smaller angles. Informally, ELS plays an important role in correcting the features’ *phase gap* between skip connections and other *homogeneous* choices (inverted bottlenecks), which turns this *heterogeneous* operation into a near-homogeneous one. As a result, for both one-shot approaches, supernets enjoy higher training accuracies (red line) and lower variances (red shaded area) as in Figure 1. There is still a small proportion of models with low accuracies, which can be easily excluded in a constrained optimization process.

6.2 Shallow Model Estimation

Scalability is made possible in a variable-depth supernet as discussed in Section 3. Still, we need to properly estimate shallow models (those with skip connections). This is hard for the supernet trained without ELS. We can easily provide an example in Table 3, where model A is underestimated with

| Methods | Resolution | Depth (\times) | Channel (\times) | $\times+$ (B) | Params (M) | Top-1 (%) | Top-5 (%) |
|---|------------------|-----------------------|-------------------------|------------------|---------------|--------------|--------------|
| DenseNet-264 [2017] | 224 \times 224 | - | - | 6 | 34 | 77.9 | 93.9 |
| Xception [2017] | 299 \times 299 | - | - | 8.4 | 23 | 79.0 | 94.5 |
| EfficientNet B2 [2019] | 260 \times 260 | 1.2 | 1.1 | 1.0 | 9.2 | 79.8 (79.4)* | 94.9 (94.7)* |
| SCARLET-A2 (ours w/o fixed AutoAugment) | 260 \times 260 | 1.0 | 1.4 | 1.0 | 12.5 | 79.5 | 94.8 |
| ResNeXt-101 [2017] | 320 \times 320 | - | - | 32 | 84 | 80.9 | 95.6 |
| PolyNet [2017] | 331 \times 331 | - | - | 35 | 92 | 81.3 | 95.8 |
| SENet [2018] | 320 \times 320 | - | - | 42 | 146 | 82.7 | 96.2 |
| EfficientNet B4 [2019] | 380 \times 380 | 1.8 | 1.4 | 4.2 | 19 | 82.6 | 96.3 |
| SCARLET-A4 (ours w/o fixed AutoAugment) | 380 \times 380 | 2.0 | 1.4 | 4.2 | 27.8 | 82.3 | 96.0 |

Table 2: Single-crop results of scaled architectures on ImageNet validation set. *: Retrained without fixed AutoAugment.

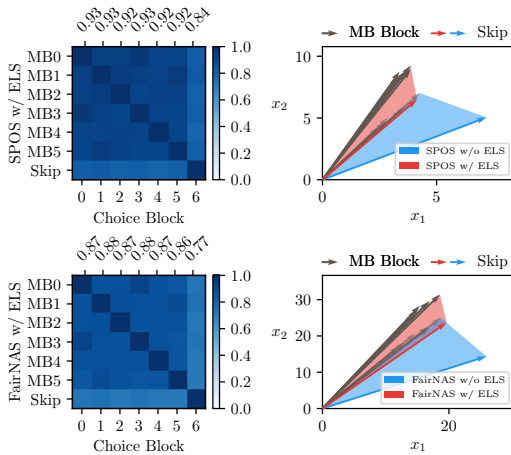


Figure 4: Cosine similarity of the third layer’s feature maps (averaged on 32 channels, shown as x -axis at the top) of 7 blocks in supernet with ELS (left). Each block’s feature vectors projected to 2-dimensional space (x_1, x_2), with their angles shadowed (right). **Top:** Single Path One-Shot [Guo *et al.*, 2019], **Bottom:** FairNAS [Chu *et al.*, 2019].

1% accuracy and B overestimated (better than A). The truth is just the opposite, A (74%) is better than B (73.3%). This is, however, correctly predicted by the supernet with ELS enabled, meaning the stabilized supernet has a better ranking ability.

6.3 Constrained Optimization

For search spaces with skip connections, to limit the minimum accuracy is more than necessary. We know that models with too many skip connections have lower multiply-adds. In a standard NSGA-II [Deb *et al.*, 2002] process, these models will be in the high-ranking non-dominated sets. An extreme case is the model consists of skip connections in all 19 layers, where it stays as a boundary node (because of minimum multiply-adds) to have an infinite crowding distance. Hence its gene never dies out. This brings in gene contamination for the evolution process. To demonstrate this issue, we compare the case with $acc_{min} = 0$ and $acc_{min} = 0.4$ in Figure 5. With the latter constraint, we can observe the appearance of skip connections has been reduced (red line at the bottom fig-

| Models (in S_1) | Top-1 (%) (w/o ELS) | Top-1 (%) (w/ ELS) | Top-1 (%) (standalone) |
|---|------------------------|-----------------------|---------------------------|
| A=(0, 5, 0, 6, 3, 2, 3, 0, 2, 1, 3, 5, 2, 4, 4, 4, 5, 3, 6) | 1.0 | 53.1 | 74.0 |
| B=(5, 0, 1, 0, 2, 6, 6, 4, 3, 1, 5, 1, 0, 2, 4, 4, 1, 1, 2) | 49.5 | 49.6 | 73.3 |

Table 3: Model A and B (represented by the order of choice blocks) from S_1 are mistakenly estimated in the supernet trained w/o ELS.

ure). As a consequence, the evolution converges to a better Pareto Front (red line at the top figure): higher validation accuracies at the same level of multiply-adds.

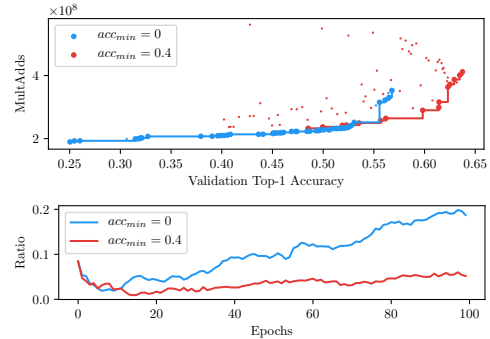


Figure 5: Ablation study on constrained optimization. **Top:** Pareto front of MultAdds vs. Accuracy. **Bottom:** The ratios of skip connections per epoch.

6.4 Visualization of Equivariant Learnable Stabilizer

To further understand what does an equivariant learnable stabilizer look like, we illustrate the weights of 1×1 convolutions from four layers at various depths (with equal input and output sizes) in Figure 6. Only the diagonal weights are activated with high values. This is just as expected. As the parameter-bearing parts of inverted bottlenecks in the same layer learn residual information, the added stabilizer should

capture an identity mapping as well. It also coincides with the discovered channel-wise similarity, the stabilizer only needs to deal with discrepancy channel by channel, which is very efficient.

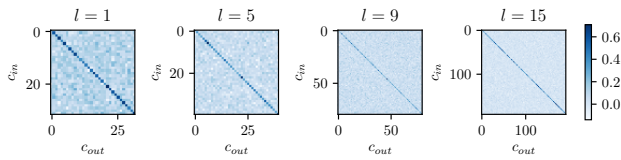


Figure 6: The visualization of ELS’s weights in different layers. The weights are mainly activated diagonally.

7 Conclusion

In this paper, we expose a critical failure in single-path one-shot neural architecture search when scalability is considered. The dissimilarity lying in the feature maps of various choice blocks hinders supernet training. To cure this, we propose a simple equivariant learnable stabilizer, which is demonstrated to be especially effective to boost similarity and in turn the supernet performance. We prove that imposing the stabilizer makes an equivalent mapping from the stabilized model to its shallow counterpart in terms of representational power. We also employ a weighted multi-objective evolutionary search, from which our final state-of-the-art SCARLET architectures are drawn. As a comparison, our method is much more efficient than unnecessarily costly EfficientNet, either for searching the baseline or upscaling the larger models.

References

- [Bender *et al.*, 2018] Gabriel Bender, Pieter-Jan Kindermans, Barret Zoph, Vijay Vasudevan, and Quoc Le. Understanding and Simplifying One-Shot Architecture Search. In *International Conference on Machine Learning*, pages 549–558, 2018.
- [Cai *et al.*, 2019] Han Cai, Ligeng Zhu, and Song Han. ProxylessNAS: Direct Neural Architecture Search on Target Task and Hardware. In *International Conference on Learning Representations*, 2019.
- [Chen *et al.*, 2019] Xin Chen, Lingxi Xie, Jun Wu, and Qi Tian. Progressive Differentiable Architecture Search: Bridging the Depth Gap between Search and Evaluation. In *International Conference on Computer Vision*, 2019.
- [Chollet, 2017] François Chollet. Xception: Deep Learning with Depthwise Separable Convolutions. In *Proceedings of the IEEE Conference on Computer Vision and Pattern Recognition*, pages 1251–1258, 2017.
- [Chu *et al.*, 2019] Xiangxiang Chu, Bo Zhang, Ruijun Xu, and Jixiang Li. FairNAS: Rethinking Evaluation Fairness of Weight Sharing Neural Architecture Search. *arXiv preprint. arXiv:1907.01845*, 2019.
- [Cubuk *et al.*, 2018] Ekin D Cubuk, Barret Zoph, Dandelion Mane, Vijay Vasudevan, and Quoc V Le. AutoAugment: Learning Augmentation Policies from Data. *arXiv preprint. arXiv:1805.09501*, 2018.
- [Deb *et al.*, 2002] Kalyanmoy Deb, Amrit Pratap, Sameer Agarwal, and TAMT Meyarivan. A Fast and Elitist Multiobjective Genetic Algorithm: NSGA-II. *IEEE Transactions on Evolutionary Computation*, 6(2):182–197, 2002.
- [Deng *et al.*, 2009] Jia Deng, Wei Dong, Richard Socher, Li-Jia Li, Kai Li, and Li Fei-Fei. ImageNet: A Large-Scale Hierarchical Image Database. In *Proceedings of the IEEE Conference on Computer Vision and Pattern Recognition*, pages 248–255. Ieee, 2009.
- [Dong and Yang, 2019] Xuanyi Dong and Yi Yang. Searching for a Robust Neural Architecture in Four GPU Hours. In *Proceedings of the IEEE Conference on Computer Vision and Pattern Recognition*, pages 1761–1770, 2019.
- [Friedrich *et al.*, 2011] Tobias Friedrich, Trent Kroeger, and Frank Neumann. Weighted Preferences in Evolutionary Multi-Objective Optimization. In *Australasian Joint Conference on Artificial Intelligence*, pages 291–300. Springer, 2011.
- [Guo *et al.*, 2019] Zichao Guo, Xiangyu Zhang, Haoyuan Mu, Wen Heng, Zechun Liu, Yichen Wei, and Jian Sun. Single Path One-Shot Neural Architecture Search with Uniform Sampling. *arXiv preprint. arXiv:1904.00420*, 2019.
- [He *et al.*, 2016] Kaiming He, Xiangyu Zhang, Shaoqing Ren, and Jian Sun. Deep Residual Learning for Image Recognition. In *Proceedings of the IEEE Conference on Computer Vision and Pattern Recognition*, pages 770–778, 2016.
- [Howard *et al.*, 2019] Andrew Howard, Mark Sandler, Grace Chu, Liang-Chieh Chen, Bo Chen, Mingxing Tan, Weijun Wang, Yukun Zhu, Ruoming Pang, Vijay Vasudevan, et al. Searching for MobileNetV3. *arXiv preprint. arXiv:1905.02244*, 2019.
- [Hu *et al.*, 2018] Jie Hu, Li Shen, and Gang Sun. Squeeze-and-Excitation Networks. In *Proceedings of the IEEE Conference on Computer Vision and Pattern Recognition*, pages 7132–7141, 2018.
- [Huang *et al.*, 2017] Gao Huang, Zhuang Liu, Laurens Van Der Maaten, and Kilian Q Weinberger. Densely Connected Convolutional Networks. In *Proceedings of the IEEE Conference on Computer Vision and Pattern Recognition*, pages 4700–4708, 2017.
- [Liu *et al.*, 2019] Hanxiao Liu, Karen Simonyan, and Yiming Yang. DARTS: Differentiable Architecture Search. In *International Conference on Learning Representations*, 2019.
- [Pham *et al.*, 2018] Hieu Pham, Melody Y Guan, Barret Zoph, Quoc V Le, and Jeff Dean. Efficient Neural Architecture Search via Parameter Sharing. In *International Conference on Machine Learning*, 2018.

- [Sandler *et al.*, 2018] Mark Sandler, Andrew Howard, Menglong Zhu, Andrey Zhmoginov, and Liang-Chieh Chen. MobileNetV2: Inverted Residuals and Linear Bottlenecks. In *Proceedings of the IEEE Conference on Computer Vision and Pattern Recognition*, pages 4510–4520, 2018.
- [Srivastava *et al.*, 2014] Nitish Srivastava, Geoffrey Hinton, Alex Krizhevsky, Ilya Sutskever, and Ruslan Salakhutdinov. Dropout: A Simple Way to Prevent Neural Networks from Overfitting. *The Journal of Machine Learning Research*, 15(1):1929–1958, 2014.
- [Stamoulis *et al.*, 2019] Dimitrios Stamoulis, Ruizhou Ding, Di Wang, Dimitrios Lymberopoulos, Bodhi Priyantha, Jie Liu, and Diana Marculescu. Single-Path NAS: Designing Hardware-Efficient ConvNets in less than 4 Hours. *arXiv preprint arXiv:1904.02877*, 2019.
- [Szegedy *et al.*, 2017] Christian Szegedy, Sergey Ioffe, Vincent Vanhoucke, and Alexander A Alemi. Inception-v4, Inception-ResNet and the Impact of Residual Connections on Learning. In *Thirty-First AAAI Conference on Artificial Intelligence*, 2017.
- [Tan and Le, 2019] Mingxing Tan and Quoc V Le. EfficientNet: Rethinking Model Scaling for Convolutional Neural Networks. In *International Conference on Machine Learning*, 2019.
- [Tan *et al.*, 2019] Mingxing Tan, Bo Chen, Ruoming Pang, Vijay Vasudevan, and Quoc V Le. Mnasnet: Platform-Aware Neural Architecture Search for Mobile. In *Proceedings of the IEEE Conference on Computer Vision and Pattern Recognition*, 2019.
- [Wu *et al.*, 2019] Bichen Wu, Xiaoliang Dai, Peizhao Zhang, Yanghan Wang, Fei Sun, Yiming Wu, Yuandong Tian, Peter Vajda, Yangqing Jia, and Kurt Keutzer. FBNet: Hardware-Aware Efficient ConvNet Design via Differentiable Neural Architecture Search. *The IEEE Conference on Computer Vision and Pattern Recognition*, 2019.
- [Xie *et al.*, 2017] Saining Xie, Ross Girshick, Piotr Dollár, Zhuowen Tu, and Kaiming He. Aggregated Residual Transformations for Deep Neural Networks. In *Proceedings of the IEEE Conference on Computer Vision and Pattern Recognition*, pages 1492–1500, 2017.
- [Zela *et al.*, 2019] Arber Zela, Thomas Elsken, Tonmoy Saikia, Yassine Marrakchi, Thomas Brox, and Frank Hutter. Understanding and Robustifying Differentiable Architecture Search. *arXiv preprint arXiv:1909.09656*, 2019.
- [Zhang *et al.*, 2017] Xingcheng Zhang, Zhizhong Li, Chen Change Loy, and Dahua Lin. PolyNet: A Pursuit of Structural Diversity in Very Deep Networks. In *Proceedings of the IEEE Conference on Computer Vision and Pattern Recognition*, pages 718–726, 2017.
- [Zhang *et al.*, 2018] Xiangyu Zhang, Xinyu Zhou, Mengxiao Lin, and Jian Sun. ShuffleNet: An Extremely Efficient Convolutional Neural Network for Mobile Devices. In *The IEEE Conference on Computer Vision and Pattern Recognition*, June 2018.
- [Zoph *et al.*, 2018] Barret Zoph, Vijay Vasudevan, Jonathon Shlens, and Quoc V Le. Learning Transferable Architectures for Scalable Image Recognition. In *Proceedings of the IEEE Conference on Computer Vision and Pattern Recognition*, pages 8697–8710, 2018.